UC San Diego
UC San Diego Previously Published Works

Title

Evaluation of cortical bone perfusion using dynamic contrast enhanced ultrashort echo time imaging: a feasibility study

Permalink

Journal

ISSN

Authors

Wan, Lidi
Wu, Mei
Sheth, Vipul
et al.

Publication Date

DOI

Peer reviewed

Evaluation of cortical bone perfusion using dynamic contrast enhanced ultrashort echo time imaging: a feasibility study

Lidi Wan[#], Mei Wu[#], Vipul Sheth, Hongda Shao, Hyungseok Jang, Graeme Bydder, Jiang Du

Department of Radiology, University of California, San Diego, CA, USA

[#]These authors contributed equally to this work.

Correspondence to: Jiang Du. Department of Radiology, University of California, 9500 Gilman Dr, San Diego, CA 92093, USA. Email: jiangdu@ucsd.edu.

Background: Dynamic contrast enhanced magnetic resonance imaging (DCE-MRI) has been used to study perfusion in a wide variety of soft tissues including the bone marrow. Study of perfusion in hard tissues such as cortical bone has been much more limited because of the lack of detectable MR signal from them using conventional pulse sequences. However, two-dimensional (2D) ultrashort echo time (UTE) sequences detect signal from cortical bone and allow fast imaging of this tissue. In addition, adiabatic 2D inversion recovery UTE (IR-UTE) sequences can provide excellent signal suppression of soft tissues, such as muscle and marrow, and allow cortical bone to be seen with high contrast and reduced artefacts. We aimed to assess the feasibility of using 2D UTE and 2D IR-UTE sequences to perform DCE-MRI in the cortical bone of rabbits and human volunteers.

Methods: Cortical bone perfusion was studied in rabbits (n=12) and human volunteers (n=3) using 2D UTE and 2D IR-UTE sequences on a clinical 3T scanner. Dynamic data with an in-plane resolution of ~0.5× 0.5 mm², single slice thickness of 3 mm for rabbits and 10 mm for human volunteers, and temporal resolution of 23 s for 2D UTE imaging of rabbits, 28 s for 2D UTE imaging of human volunteers, and 60 s for 2D IR-UTE imaging of both the rabbits and human volunteers were acquired before and after the injection of a Gd contrast agent (Gd-BOPTA: Multihance; Bracco Imaging SpA, Milan, Italy). The dose was 0.06 mmol/kg for rabbits and 0.2 mmol/kg for human subjects. Kinetic analyses based on the Brix model, as well as simple calculations of maximum enhancement (ME) and enhancement slope (ES), were performed.

Results: The 12 rabbits showed a mean K^{trans} of 0.36 ± 0.07 min^{-1}, K_{ep} of 8.42 ± 3.17 min^{-1}, ME of 28.30 ± 6.83, ES of 0.35 ± 0.18 for the femur with the 2D UTE sequence, and a mean K^{trans} of 0.45 ± 0.10 min^{-1}, K_{ep} of 9.80 ± 0.50 min^{-1}, ME of 48.84 ± 12.12, and ES of 0.69 ± 0.27 for the femur with the 2D IR-UTE sequence. Lower ME and ES values were observed in the tibial midshaft of healthy human volunteers compared to rabbits.

Conclusions: These results show that 2D UTE and 2D IR-UTE sequences are capable of detecting dynamic contrast enhancement in cortical bone in both rabbits and healthy human volunteers. Clinical studies with these techniques are likely to be feasible.

Keywords: ultrashort echo time (UTE); inversion recovery UTE (IR-UTE); cortical bone; T1; T2*; perfusion

Introduction

Bone is divided into trabecular and cortical components which are both highly vascularized (1). All trabecular bone, and the inner two-thirds of cortical bone receive their blood supply via the marrow cavity (2). The outer third of cortical bone receives its perfusion from the periosteum.

1384

Wan et al. Cortical bone perfusion assessed by UTE DCE-MRI

Perfusion plays an important role in bone growth and development as well as in disease and bone healing. Several magnetic resonance imaging (MRI) studies have focused on perfusion in the bone marrow in diseases of bone including osteoporosis, osteoarthritis, and multiple myeloma (2-5). Bone marrow perfusion is reduced in osteoporotic trabecular bone (6); this decreased vascularity may contribute to an increase in fracture risk (7). Reduced marrow perfusion occurs in synchrony with reduced bone mineral in vertebral trabecular bone (8).

Most MRI studies of bone perfusion have involved bone marrow; there have been no MRI studies of perfusion in trabecular bone and very little has been published about perfusion in cortical bone, despite the fact that cortical bone comprises about 80% of the bone mass of the body.

Dynamic contrast enhanced magnetic resonance imaging (DCE-MRI) is a powerful technique which provides *in vivo* assessment of the microvascular properties of various lesions, such as cerebral infarction and brain tumors (9). Usually the technique requires acquisition of dynamic MRI signals over a region of interest (ROI) following the injection of a gadolinium-based contrast agent, using fast gradient echo sequences with typical echo times (TEs) of several milliseconds or longer. This is usually performed in tissues with T2s of several, or many milliseconds. DCE-MRI of cortical bone has not been amenable to study using this approach due to its extremely short T2* of approximately 0.3 to 0.5 ms (10) which results in no detectable signal from this tissue either without or with the addition of a contrast agent.

With the advent of two-dimensional (2D) ultrashort echo time (UTE) MRI sequences with TEs typically 100 times or more shorter than those of conventional clinical gradient echo sequences, signal from cortical bone can be detected. In principle this could allow study of perfusion in cortical bone (10-13). However, 2D UTE sequences are subject to eddy currents and out-of-slice signal contamination which may distort DCE curves during evaluation of perfusion in cortical bone, especially for small animals such as rabbits, rats and mice. 2D inversion recovery UTE (IR-UTE) sequences have been used for high contrast imaging of cortical bone because, in addition to detecting signal from the bone, they can provide excellent suppression of long T2 signals from muscle and marrow (14). This may be important for the study of perfusion in cortical bone in order to avoid artifactual high signals from long T2 muscle and marrow contaminating contrast enhancement curves in cortical bone. The purpose of this study was to assess the feasibility of using both 2D

UTE and 2D IR-UTE sequences on a clinical 3T scanner to demonstrate perfusion in the cortical bone of rabbits and healthy human volunteers.

Methods

Subjects

Twelve 6-month-old female New Zealand white rabbits were studied under protocols approved by the IACUC of the University of California, San Diego (UCSD). The rabbits were randomly divided into two groups (six in each group) and imaged with 2D UTE and 2D IR-UTE sequences respectively (details below). Three healthy human volunteers (male: 38, 40, and 68 years old) were recruited for this part of the study which focused on the tibial midshaft. All studies were approved by the UCSD Institutional Review Board (IRB) and informed consent was obtained from each human subject.

Pulse sequences

All MRI experiments were performed on a Signa 3T scanner (GE Healthcare, Milwaukee, WI, USA). A 7.6 cm diameter surface coil was used to improve the image signal to noise ratio (SNR). The basic 2D UTE pulse sequence employed two half radiofrequency excitations followed by radial ramp sampling (*Figure 1A*). A complete slice profile was generated by collecting data with the slice selection gradient in one direction and adding this to data collected with the polarity of the slice selection gradient reversed. In 2D IR-UTE imaging (*Figure 1B*), an adiabatic fast passage (Silver Hoult) inversion pulse (pulse duration =8.64 ms) was added as a preparation pulse before the 2D UTE data acquisition. Clinical 2D gradient recalled echo (GRE) sequences were also performed for comparison.

MR data acquisition

All the UTE imaging parameters are summarized in *Table 1*. The rabbit study used a small field of view (FOV) of 6 cm, a thin slice of 3 mm, and an acquisition matrix of 128×128, whereas the human study used a large FOV of 12–15 cm, a thick slice of 10 cm, and an acquisition matrix of 320×320 for the UTE, and 256×256 for the IR-UTE acquisitions. Other imaging parameters, including the repetition time (TR), TE, inversion time (TI), number of projections, flip angle (FA), bandwidth (BW), and number of excitations
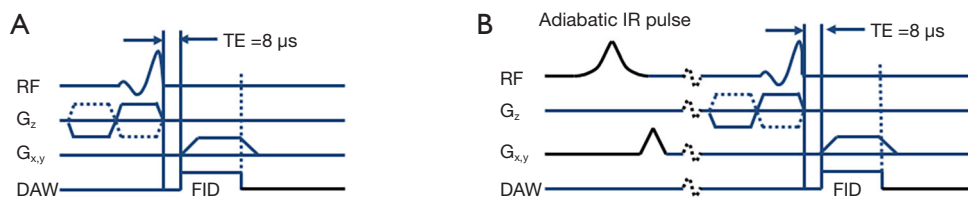
Figure 1 Pulse sequence for 2D UTE imaging using half pulse excitation, radial center-out trajectory, and ramp sampling with a minimal nominal TE of 8 µs (A); an adiabatic IR preparation pulse was applied before the regular 2D UTE acquisitions to suppress signals from long T2 muscle and marrow providing high contrast imaging of cortical bone using 2D IR-UTE imaging (B). 2D UTE, two-dimensional ultrashort echo time; TE, echo time; IR, inversion recovery.

Table 1 The imaging protocols for 2D UTE and 2D IR-UTE imaging of rabbits and human volunteers, respectively. The scan time for a single slice 2D UTE or 2D IR-UTE image is the temporal resolution

MRI sequences	TR (ms)	TE (µs)	TI (ms)	FOV (cm)	Thick (mm)	Matrix	#Proj	Filp angle	BW (kHz)	NEX	Temporal resolution (s)
Rabbit study											
UTE	29	8	–	6	3	128×128	403	35°	62.5	2	23
IR-UTE	300	8	110	6	3	128×128	101	60°	62.5	2	60
Human study											
UTE	20	8	–	15	10	320×320	711	35°	250	2	28
IR-UTE	300	8	110	15	10	256×256	101	60°	250	2	60

2D UTE, two-dimensional ultrashort echo time; IR-UTE, inversion recovery UTE; MRI, magnetic resonance imaging; TR, repetition time; TE, echo time; TI, inversion time; FOV, field of view; #Proj, number of projections; BW, bandwidth; NEX, number of excitations.

(NEX) are listed in *Table 1*. A single axial slice was acquired with the imaging plane perpendicular to the femoral midshaft in order to minimize partial volume effects. The number of projections was adjusted to reduce streaking artifacts, and increase both SNR and temporal resolution. The temporal resolution was 23 s for 2D UTE imaging of rabbits, 28 s for 2D UTE imaging of human volunteers, and 60 s for 2D IR-UTE imaging in both the rabbits and human volunteers.

All the rabbits were anesthetized with intramuscular injections of 3% soluble pentobarbitone (1.0 mg/kg; Sigma, USA). Each rabbit was placed on a homemade plastic holder which also held the 7.6 cm diameter surface coil. The same coil was used in all the human volunteer studies. A single axial slice was acquired from the femur of the rabbits and from the tibial midshaft of the human volunteers. Contrast injection was conducted via a marginal ear vein in the rabbits and a forearm vein in the human volunteers. A low molecular weight Gd contrast agent (Gd-BOPTA: Multihance; Bracco Imaging SpA, Mila, Italy) was used. The dose was 0.06 mmol/kg for the rabbits, and 0.2 mmol/kg

for the human subjects. Five to ten acquisitions were collected before contrast agent injection as a baseline. After injection the MR data acquisitions with the 2D UTE or 2D IR-UTE sequences were repeated for up to 60 min.

MR data analysis

All the acquired images were analyzed using Matlab 2013A (Mathworks, Natick, MA). A custom-made fitting algorithm was coded under Mathematica (Wolfram Research Inc., IL, USA), which treats both the kinetic model and MRI signal model together. With this approach MRI noise is propagated into the values of the pharmacokinetic parameters so that overall uncertainty can be estimated and correlations can be performed. The dynamic data were processed using a pharmacokinetic Brix model (15), which has advantages over the Tofts model for data fitting (16). ROIs in cortical bone as well as an adjacent artery [to obtain an arterial input function (AIF)] were manually selected so that perfusion of cortical bone could be compared with arterial blood changes. Four ROIs were placed in four

1386

Wan et al. Cortical bone perfusion assessed by UTE DCE-MRI
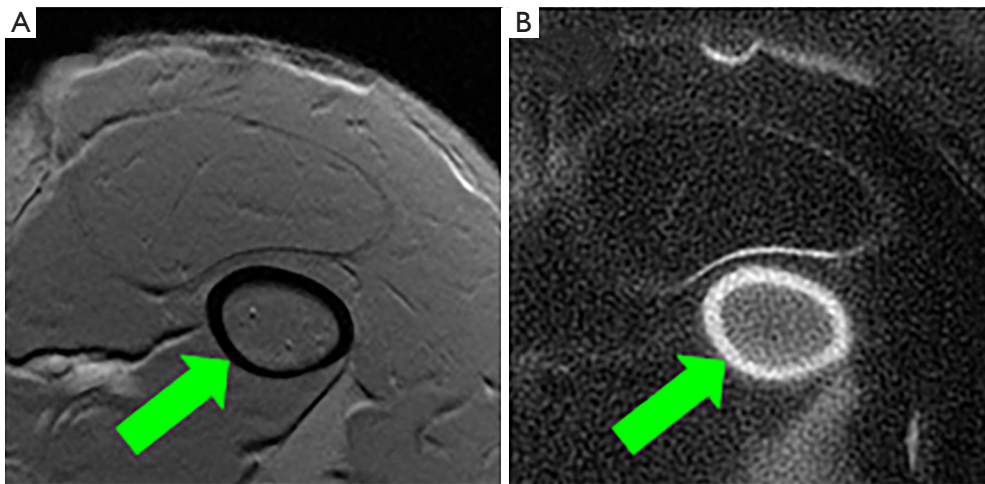
Figure 2 The femur of a rabbit imaged with clinical 2D GRE sequence (A) and 2D IR-UTE sequence (B). (A) The clinical GRE sequence shows a signal void in the femur (arrow), while the (B) 2D IR-UTE sequence shows high signal and contrast in the rabbit femur (arrow). 2D GRE, two-dimensional gradient recalled echo; IR-UTE, inversion recovery ultrashort echo time.

different regions (anterior, posterior, left and right) of cortical bone. These regions avoided bone boundaries in order to minimize partial volume and other artifacts from adjacent muscle and marrow.

A blood baseline T1 of 1,400 ms and tibial cortex baseline T1 of 220 ms were assumed for kinetic analysis. Parameters including K^{trans} and K_{ep} were calculated (4). K^{trans} reflects the size of the extravascular extracellular space that the contrast agents can penetrate, while K_{ep} and the slope of the enhancement curve reflect the speed of contrast agent entry and wash out. Maximum enhancement (ME) and enhancement slope (ES) were calculated for further evaluation of cortical bone perfusion using the technique described by Griffith *et al.* (17). ME was calculated as the signal difference between maximal and minimal bone signal divided by the baseline signal. ES was calculated as the difference between maximal signal and baseline signal divided by the baseline signal, and further divided by the time interval between the two time points at which the minimal and maximal signal intensities of interest were reached (10% and 90% of the maximum signal intensity respectively). Both parameters were derived from the first-pass phase of contrast enhancement and reflected the arrival of the contrast agent into the arteries and capillaries of cortical bone as well as its diffusion into the extracellular space and subsequent departure (17). The derived parametric perfusion data from 2D UTE and 2D IR-UTE sequences were presented as means and standard deviations

(SDs) over the multiple ROIs.

Results

The feasibility of high contrast UTE imaging of cortical bone is demonstrated in *Figure 2*, which shows imaging of the femur of a rabbit using 2D GRE (*Figure 2A*) and 2D IR-UTE (*Figure 2B*) sequences. The 2D GRE sequence shows a signal void in the cortex of the femur (arrow), with high signal from surrounding muscle and bone marrow. The 2D IR-UTE sequence shows high signal in the cortex of the femur (arrow), with excellent suppression of muscle and marrow signals.

Representative 2D UTE imaging of the femur of a rabbit at three typical time points (pre-contrast, peak, and post-contrast enhancement), as well as the contrast enhancement curves for ROIs drawn in the adjacent artery and femur, respectively, are shown in *Figure 3*. The 2D UTE image shows little contrast difference in the femur due to high signal from surrounding muscle and marrow. During peak enhancement, vessels are enhanced more than three-fold, with slight enhancement in the muscle and about 25% enhancement in the femur. However, the contrast enhancement in the femur appears "invisible" due to its low signal relative to the surrounding soft tissues before and after enhancement. The femur remained up to 20% enhanced about 15 min after contrast injection.

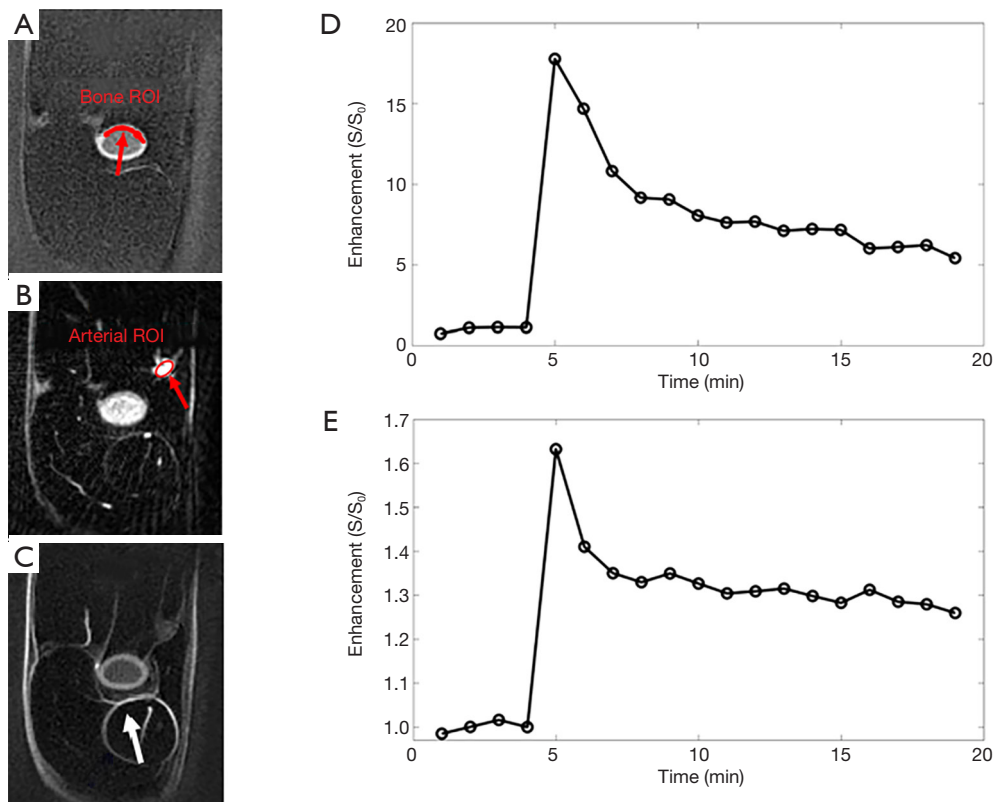Representative 2D IR-UTE imaging of the femur of
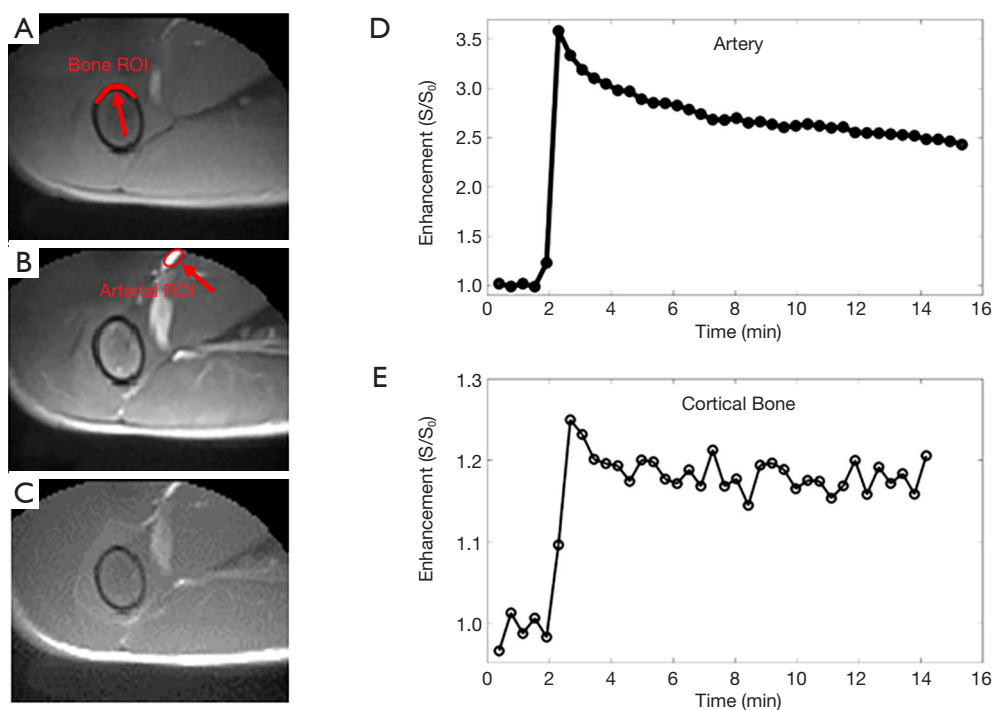
Figure 3 Pre-contrast (A), peak enhancement (B), and post-contrast (C) 2D UTE images of a rabbit, as well as the contrast enhancement curves for ROIs drawn in the adjacent artery (D) and femoral midshaft (E), respectively. The femur showed a maximum enhancement value of around 25% and a post-enhancement value of around 20%, while the artery showed a maximum enhancement of around 250%. ROI, region of interest; 2D UTE, two-dimensional ultrashort echo time.

a rabbit at three typical time points (pre-contrast, peak, and post-contrast enhancement), as well as the contrast enhancement curves for ROIs drawn in the adjacent artery and the femur, respectively, are shown in *Figure 4*. Signals from muscle and marrow are suppressed on the pre- and post-contrast images. Higher signal was observed in the marrow during peak enhancement, largely due to the high contrast agent concentration which greatly shortened its T1, leading to a high signal with 2D IR-UTE imaging. Signal enhancement in the femur, as well as in aponeuroses, is obvious in the post-contrast 2D IR-UTE images. On these images blood in the artery has an enhancement of more than 15-fold, relative to its inverted and partially nulled pre-contrast signal. The femur cortical bone has a peak enhancement of about 60% and about 30% enhancement at 20 min after contrast injection.

Perfusion parameters from kinetic analyses based on the Brix model for the 12 rabbits imaged with 2D UTE and 2D IR-UTE sequences, respectively, are shown in *Table 2*. A mean K^{trans} of 0.36 ± 0.07 min^{-1}, K_{ep} of 8.42 ± 3.17 min^{-1}, ME of 28.30 ± 6.83, and ES of 0.35 ± 0.18 were observed

for the femur with the 2D UTE sequence, while a mean K^{trans} of 0.45 ± 0.10 min^{-1}, K_{ep} of 9.80 ± 0.50 min^{-1}, ME of 48.84 ± 12.12, and ES of 0.69 ± 0.27 were observed for the femur with the 2D IR-UTE sequence. Higher perfusion parameters, especially ME and ES, were observed in the femur with the 2D IR-UTE sequence, which was expected as baseline soft tissue and bone signal are partially or wholly suppressed by the adiabatic IR preparation pulse, leading to greater contrast enhancement relative to this reduced signal.

Representative 2D UTE images of the tibial midshaft of a 38-year-old healthy volunteer pre-injection and at the peak of bone enhancement are shown in *Figure 5*. The local coil used for MRI signal detection improves SNR, but also produces non-uniform sensitivity, which is evident on *Figure 5A*. For better visualization of detail, average pre-injection data were subtracted from the post-injection image in *Figure 5B*. The AIF and bone ROIs are shown in *Figure 5B* with a red arrow and a red ellipse, respectively. The corresponding kinetic analyses are also displayed. K^{trans} and K_{ep} were estimated with a reasonably low error.

1388

Wan et al. Cortical bone perfusion assessed by UTE DCE-MRI

Figure 4 Pre-contrast (A), peak enhancement (B), and post-contrast (C) 2D IR-UTE images of a rabbit, as well as the contrast enhancement curves for ROIs drawn in the adjacent artery (D) and femoral midshaft (E). On the 20 min post-contrast image (C), there is highlighting of the aponeuroses (arrow) of the leg, which are not so apparent in the pre-contrast scan. ROI, region of interest; 2D IR-UTE, two-dimensional inversion recovery ultrashort echo time.

Table 2 The mean and standard variation of pharmacokinetic parameters, K^{tran}, and K_{ep} as well as ME and ES of the enhancement curve accessed by 2D UTE and 2D IR-UTE imaging of the femur in rabbits

Pharmacokinetic parameters	UTE	IR-UTE
K^{tran} (min^{-1})	0.36±0.07	0.45±0.10
K_{ep} (min^{-1})	8.42±3.17	9.80±0.50
ME (%)	28.30±6.83	48.84±12.12
ES (%/s)	0.35±0.18	0.69±0.27

2D UTE, two-dimensional ultrashort echo time; IR-UTE, inversion recovery UTE; ME, maximum enhancement; ES, enhancement slope.

Representative 2D UTE and 2D IR-UTE imaging of the tibial midshaft of two human volunteers aged 68 and 40 years, respectively, at three typical time points (pre-contrast, peak, and post-contrast), as well as the corresponding bone perfusion curves are shown in *Figure 6*. 2D IR-UTE pre-contrast images show good contrast for cortical bone. 40 min after contrast injection, images show high contrast visualization of aponeuroses. 2D IR-UTE perfusion in the two volunteers show different patterns for the 68-year-old and the 40-year-old subject. The 40-year-old shows a curve with an early peak, a rapid decline and then a plateau. The curve in the 68-year-old is less peaked. In both volunteers, 2D UTE imaging shows much higher signal from muscle and marrow compared to cortical bone, and the perfusion curve shows a different pattern compared with that obtained from 2D IR-UTE imaging. *Figure 7* shows perfusion curves for both volunteers, using global ROIs for cortical bone, as well as the AIF, contrast enhancement, and ES, respectively. The younger volunteer shows higher contrast enhancement with a higher ES. Lower enhancement and slower perfusion were observed
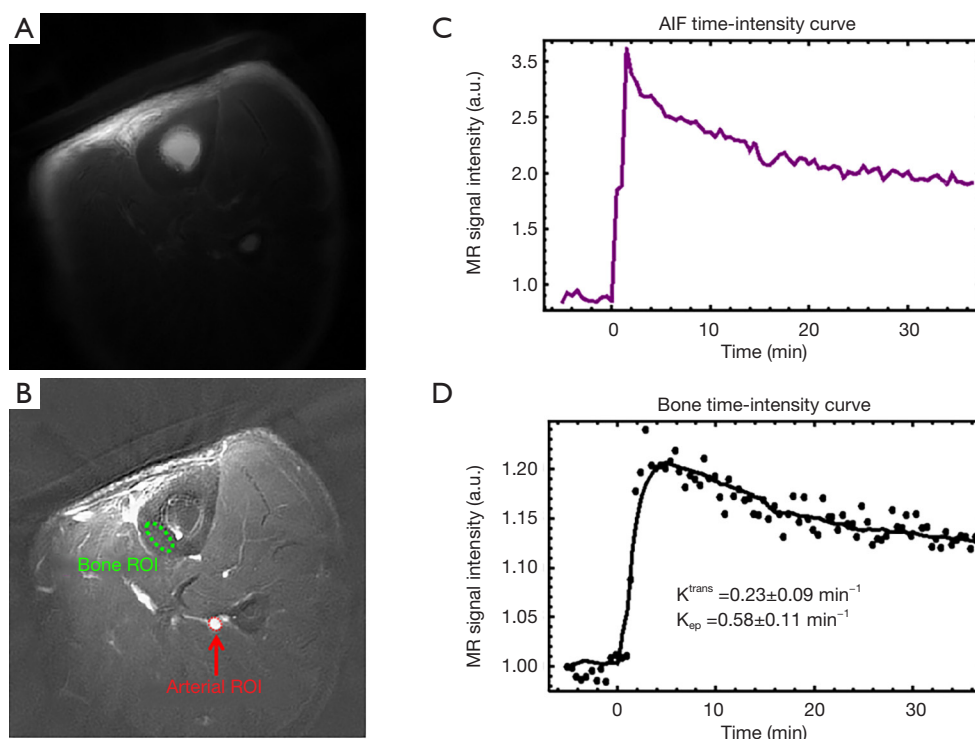
Figure 5 2D UTE imaging of the tibial midshaft of a 38-year-old healthy volunteer: pre-enhancement image (A), subtraction of the peak-from pre-enhancement image (B), contrast enhancement curve for an arterial ROI (C), and bone ROI (D). Kinetic analysis shows a K^{trans} of 0.23 min^{-1} and K_{ep} of 0.58 min^{-1}. ROI, region of interest; AIF, arterial input function; 2D UTE, two-dimensional ultrashort echo time.

in the tibial midshafts of the volunteers compared with the femurs of the rabbits.

Discussion

Various studies have shown a relationship between bone perfusion, bone remodeling and fracture repair (17-29). Increased cortical bone turnover and inflammation are associated with increased blood flow (23). There is also a strong correlation between bone perfusion and bone mineral density (BMD) (24-27). However, the nature of cortical bone makes it difficult to investigate perfusion with MRI (28), because the MRI techniques used in most soft tissue studies are not effective when applied to bone (28). UTE-type sequences make it possible to directly evaluate perfusion in cortical bone by reducing TEs from the several milliseconds of conventional sequences down to milliseconds for 2D UTE sequences (e.g., 8 µs in our study).

Cortical bone perfusion can also be assessed with nuclear medicine-based techniques, such as 18F-Fluoride positron

emission tomography (PET) (29). However, 18F-Fluoride PET is expensive, has a low spatial resolution and subjects the patient to ionizing radiation. MRI can provide much higher spatial resolution without ionizing radiation.

The 2D UTE sequence with a minimal nominal TE of 8 µs enables detection of signal from cortical bone before it decays to near zero level. In addition, the 2D IR-UTE sequence suppresses signals from long T2 muscle and marrow fat, providing high resolution and high contrast imaging of cortical bone (14). Contrast agent dynamics can be evaluated using the 2D UTE and 2D IR-UTE sequences. 2D UTE and 2D IR-UTE sequences are sensitive to eddy currents, which can lead to out-of-slice signal contamination (30). 2D IR-UTE sequences may be preferred for assessing perfusion because they suppress high out-of-slice signals from marrow and muscle and reduce this problem. This may be particularly important in imaging cortical bone in small animals such as rabbits, and more particularly rats and mice. Signals from long T2 muscle and marrow fat are generally much higher than those from cortical bone (13). Out-of-slice

1390

**Wan et al. Cortical bone perfusion assessed by UTE DCE-MRI**
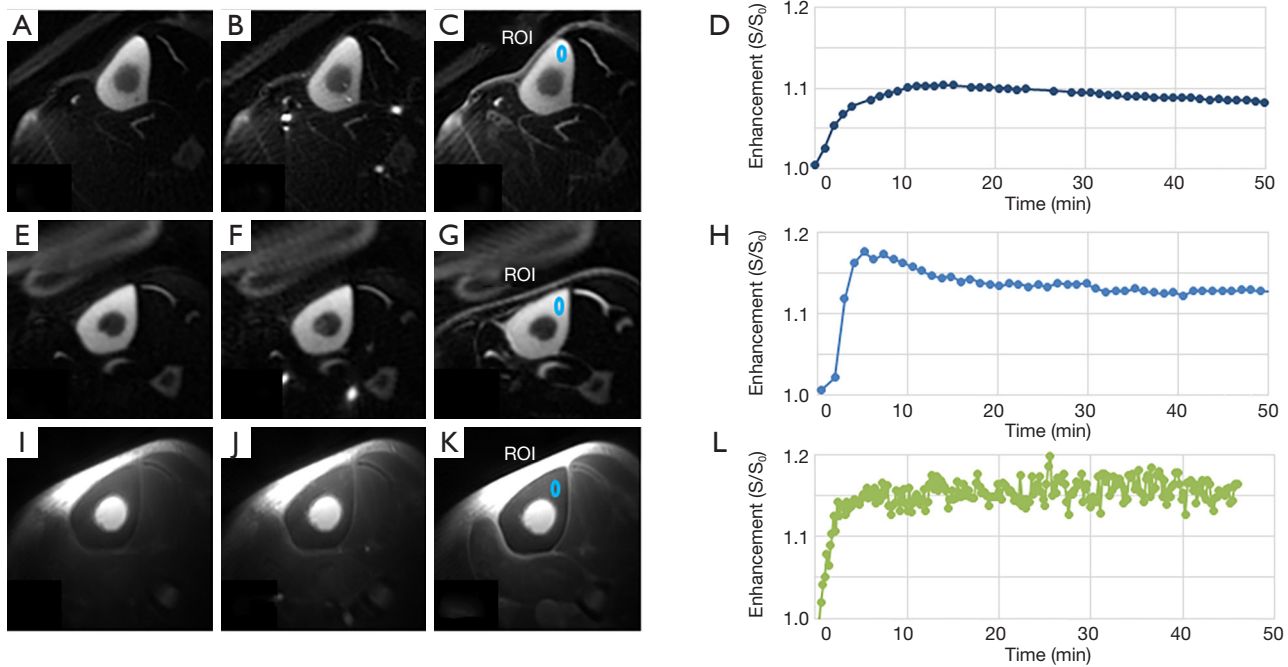
Figure 6 Pre-contrast (A,E), peak enhancement (B,F), and post-contrast (C,G) 2D IR-UTE images of two volunteers aged 68 and 40 years old, respectively, and the corresponding bone perfusion curves (D,H) derived from two small ROIs shown in (C,G). 2D UTE images of pre-contrast (I), peak-enhancement (J), and post-contrast (K), as well as the corresponding bone perfusion curve (L) are also shown for the 40-year-old volunteer. 2D IR-UTE images show high contrast visualization of cortical bone, while 2D UTE images show low contrast visualization of cortical bone. The contrast enhancement patterns are different for the two volunteers and for the two different sequences. ROI, region of interest; 2D IR-UTE, two-dimensional inversion recovery ultrashort echo time.

signal contamination may significantly distort contrast dynamic curves. We observed signal enhancement of more than 300% for cortical bone of rats when using 2D UTE sequences (results not shown), while the signal enhancement was typically less than 80% for rabbits and 20% for healthy human volunteers. The high signal enhancement observed in cortical bone in this situation is likely to be mainly due to out-of-slice soft tissue signal contamination, leading to significant overestimation of bone perfusion. For small animals such as rats and mice, the 2D IR-UTE sequence is recommended for perfusion studies of cortical bone to reduce this problem.

Our results show that perfusion in cortical bone is lower than that in marrow (6,17,18). Griffith *et al.* investigated marrow perfusion in 42 healthy men, 17 men with OP, and 23 men with osteopenia, and reported a mean ME of (28.8±11.2)% and mean ES of (1.14±0.5)%/s (17). Furthermore, they found significantly decreased vertebral marrow perfusion indexes in osteoporotic subjects (mean ME: 23.52%; mean ES: 0.78%/s) compared with those in

osteopenic subjects (mean ME: 28.36%; mean ES: 1.15%/s) and those in normal subjects (mean ME: 34.49%; mean ES: 1.48%/s). Those values were much higher than the perfusion indexes for cortical bone in healthy volunteers. Much higher perfusion indexes were observed in rabbits than in human volunteers.

Recent studies suggest that cortical and trabecular bone water exists in the form of pore water residing in the macroscopic pores and water bound to the organic matrix (31). It is likely that the dynamic contrast enhancement patterns are different for these two water pools. The adiabatic IR pulse can suppress not only signals from long T2 soft tissues like muscle and marrow, but also signals from pore water in cortical bone. After contrast agent arrival, pore water T1 is reduced, leading to a fast recovery after the adiabatic IR pulse. As a result, the IR-UTE signal enhancement in cortical bone shown in *Figure 4E* (~60%) is much greater than the UTE signal enhancement shown in *Figure 3E* (~25%). Furthermore, the 2D IR-UTE sequence can potentially detect contrast enhancement in
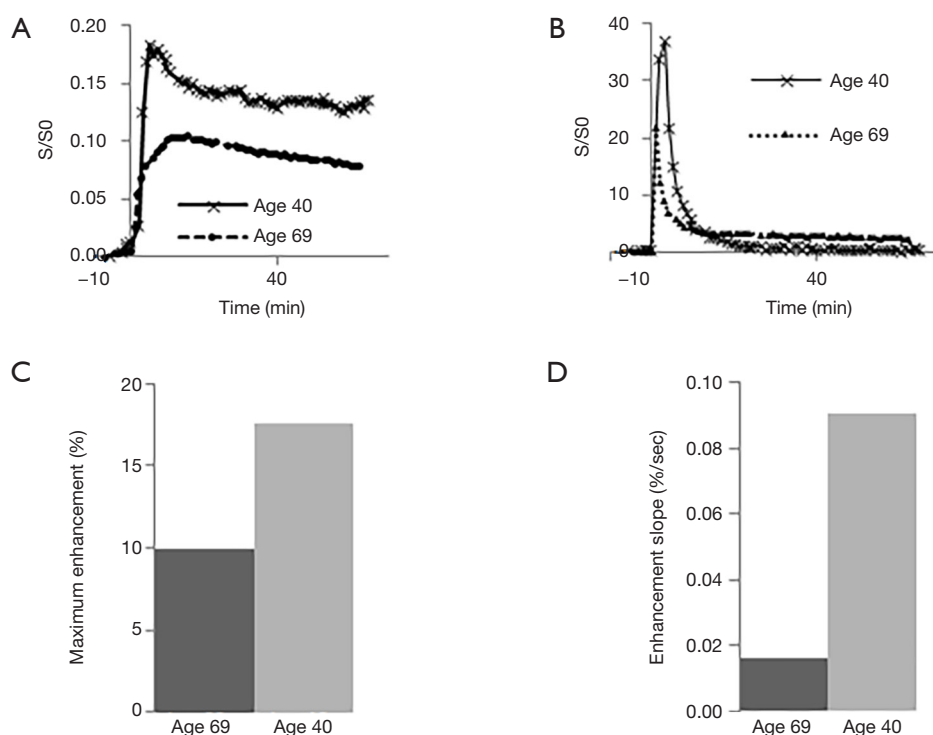
Figure 7 Global contrast enhancement curves for tibial midshaft (A), AIF (B), maximum enhancement (C), and enhancement slope (D) of the 68-year-old and 40-year-old volunteers, respectively, based on 2D IR-UTE imaging. The 40-year-old volunteer shows an early peak with a rapid decline and then a plateau, with higher maximum enhancement and enhancement slope than the 68-year-old volunteer, who shows a flatter contrast enhancement curve. AIF, arterial input function; 2D IR-UTE, two-dimensional inversion recovery ultrashort echo time.

the organic matrix, especially after contrast agent clearance from the blood and pore water compartments. The delayed enhancement in 2D IR-UTE imaging may be largely due to persistent contrast agent bound to the organic matrix. This unique technical capability may help with the development of a new iron or Gd based molecular T1 shortening agents targeting osteoclast or osteoblast activity similar to the approach used with delayed Gd-enhanced MRI of cartilage (dGEMRIC) technique (32).

There are several limitations to our study. First, the sample size is very small, with only 12 rabbits and three healthy human volunteers. Second, we only showed the feasibility of assessing perfusion in the cortical bone of rabbits and healthy human volunteers using 2D UTE and 2D IR-UTE techniques. The capability of these techniques for evaluating the relation between cortical bone perfusion and bone remodeling as well as fracture repair is important, and remains to be studied. Third, the 2D UTE sequence employs two half pulse excitations with opposite slice selective gradient polarities. Gradient

profile distortion leads to out-of-slice signal contamination, producing an imperfect slice profile. Corrections of the residual slice selection gradients and time varying main field B_0 (t) can be used to reduce out-of-slice signal contamination (30). Fourth, substantially higher perfusion indexes were observed in the rabbits compared with human volunteers, however, no histologic data were acquired to support this conclusion. More research is needed to verify and understand the difference. Fifth, the scan-rescan reproducibility of the 2D UTE and 2D IR-UTE sequences is affected by their relatively high sensitivity to eddy currents. We repeated the pre-contrast imaging over at least five time frames, and the signal oscillation was very small for arterial blood as can be seen from *Figures 3D,4D, 5D,7A,B*. However, more oscillation was observed for cortical bone, as shown in *Figures 3E,4E,5D,7A,B*, which is likely due to the much lower SNR seen in cortical bone and therefore higher sensitivity to imperfect slice profiles associated with the half-pulse excitations used in 2D UTE imaging. Sixth, 3D UTE and 3D IR-UTE imaging

1392

Wan et al. Cortical bone perfusion assessed by UTE DCE-MRI

techniques allow volumetric imaging of cortical bone with reduced eddy current artifacts and may provide more robust evaluation of perfusion in cortical bone. Further research is needed. Finally, the accuracy and influence of temporal resolution in determining pharmacokinetic parameters from dynamic 2D UTE and 2D IR-UTE imaging of cortical bone were not investigated in this study. Previous studies have demonstrated that more accurate perfusion modeling can be achieved with higher temporal resolutions (33,34). However, it is challenging to achieve high temporal resolution for bone imaging due to the requirement for two excitations with 2D UTE and 2D IR-UTE imaging, the inefficiency in covering k-space with radial sampling (more spokes are required to fill k-space satisfying the Nyquist criteria), and the inherent low SNR of cortical bone imaging due to its low water proton density and extremely short T2* (13). More research is needed to determine the optimal temporal resolution for bone perfusion studies using 2D UTE and 2D IR-UTE, as well as the 3D versions of these sequences.

In conclusion, our preliminary results show that the 2D UTE and 2D IR-UTE sequences are able to detect the DCE in cortical bone of both rabbits and healthy volunteers. Perfusion parameters for cortical bone can be derived from this data. Clinical studies using this approach appear to be feasible.

Footnote

Conflicts of Interest: The authors have no conflicts of interest to declare.

Ethical Statement: All studies were approved by the UCSD Institutional Review Board and informed consent was obtained from each human subject.

References

1. Sider KL, Song J, Davies JE. A new bone vascular perfusion compound for the simultaneous analysis of bone and vasculature. Microsc Res Tech 2010;73:665-72.

2. Ma HT, Griffith JF, Zhao X, Lv H, Yeung DK, Leung PC. Relationship between marrow perfusion and bone mineral density: a pharmacokinetic study of DCE-MRI. Conf Proc IEEE Eng Med Biol Soc 2012;2012:377-9.

3. Zhu J, Xiong Z, Zhang J, Qiu Y, Hua T, Tang G. Comparison of semi-quantitative and quantitative dynamic contrast-enhanced MRI evaluations of vertebral marrow perfusion in a rat osteoporosis model. BMC Musculoskelet Disord 2017;18:446.

4. Seah S, Wheaton D, Li L, Dyke JP, Talmo C, Harvey WF, Hunter DJ. The relationship of tibial bone perfusion to pain in knee osteoarthritis. Osteoarthritis Cartilage 2012;20:1527-33.

5. Merz M, Ritsch J, Kunz C, Wagner B, Sauer S, Hose D, Moehler T, Delorme S, Goldschmidt H, Zechmann C, Hillengass J. Dynamic contrast-enhanced magnetic resonance imaging for assessment of antiangiogenic treatment effects in multiple myeloma. Clin Cancer Res 2015;21:106-12.

6. Wang YX, Griffith JF, Kwok AW, Leung JC, Yeung DK, Ahuja AT, Leung PC. Reduced bone perfusion in proximal femur of subjects with decreased bone mineral density preferentially affects the femoral neck. Bone 2009;45:711-5.

7. Biffar A, Sourbron S, Dietrich O, Schmidt G, Ingrisch M, Reiser MF, Baur-Melnyk A. Combined diffusion-weighted and dynamic contrast-enhanced imaging of patients with acute osteoporotic vertebral fractures. Eur J Radiol 2010;76:298-303.

8. Zhu J, Zhang L, Wu X, Xiong Z, Qiu Y, Hua T, Tang G. Reduction of Longitudinal Vertebral Blood Perfusion and Its Likely Causes: A Quantitative Dynamic Contrast-enhanced MR Imaging Study of a Rat Osteoporosis Model. Radiology 2017;282:369-80.

9. Jain R. Measurements of tumor vascular leakiness using DCE in brain tumors: clinical applications. NMR Biomed 2013;26:1042-9.

10. Robson MD, Gatehouse PD, Bydder M, Bydder GM. Magnetic resonance: an introduction to ultrashort TE (UTE) imaging. J Comput Assist Tomogr 2003;27:825-46.

11. Robson MD, Gatehouse PD, So PW, Bell JD, Bydder GM. Contrast enhancement of short T2 tissues using ultrashort TE (UTE) pulse sequences. Clin Radiol 2004;59:720-6.

12. Reichert IL, Robson MD, Gatehouse PD, He T, Chappell KE, Holmes J, Girgis S, Bydder GM. Magnetic resonance imaging of cortical bone with ultrashort TE (UTE) pulse sequences. Magn Reson Imaging 2005;23:611-8.

13. Du J, Bydder GM. Qualitative and quantitative ultrashort-TE MRI of cortical bone. NMR Biomed 2013;26:489-506.

14. Li S, Ma L, Chang EY, Shao H, Chen J, Chung CB, Bydder GM, Du J. Effects of inversion time on inversion recovery prepared ultrashort echo time (IR-UTE) imaging of bound and pore water in cortical bone. NMR Biomed 2015;28:70-8.

15. Lee JH, Dyke JP, Ballon D, Ciombor DM, Rosenwasser MP, Aaron RK. Subchondral fluid dynamics in a model of osteoarthritis: use of dynamic contrast-enhanced magnetic resonance imaging. Osteoarthritis Cartilage 2009;17:1350-5.

16. Andersen EK, Hole KH, Lund KV, Sundfør K, Kristensen GB, Lyng H, Malinen E. Pharmacokinetic parameters derived from dynamic contrast enhanced MRI of cervical cancers predict chemoradiotherapy outcome. Radiother Oncol 2013;107:117-22.

17. Griffith JF, Yeung DK, Antonio GE, Lee FK, Hong AW, Wong SY, Lau EM, Leung PC. Vertebral bone mineral density, marrow perfusion, and fat content in healthy men and men with osteoporosis: dynamic contrast-enhanced MR imaging and MR spectroscopy. Radiology 2005;236:945-51.

18. Wang YX, Griffith JF, Deng M, T Ma H, Zhang YF, Yan SX, Ahuja AT. Compromised perfusion in femoral head in normal rats: distinctive perfusion MRI evidence of contrast washout delay. Br J Radiol 2012;85:e436-41.

19. Hawkins RA, Choi Y, Huang SC, Hoh CK, Dahlbom M, Schiepers C, Satyamurthy N, Barrio JR, Phelps ME. Evaluation of the skeletal kinetics of fluorine-18-Fluoride ion with PET. J Nucl Med 1992;33:633-42.

20. Carnevale V, Dicembrino F, Fruscinate V, Chiodini I, Minisola S, Scillitani A. Different patterns of global and regional skeletal uptake of 99mTc-Methylene diphosphonate with age: relevance to the pathogenesis of bone loss. J Nucl Med 2000;41:1478-83.

21. Reeve J, Arlot M, Wootton R, Edouard C, Tellez M, Hesp R, Green JR, Meunier PJ. Sleletal blood flow, iliac histomorphometry, and strontium kinetics in osteoporosis: a relationship between blood flow and corrected apposition rate. J Clin Endocrinol Metab 1988;66:1124-31.

22. Colleran PN, Wilkerson MK, Bloomfield SA, Suva LJ, Turner RT, Delp MD. Alternations in skeletal perfusion with simulated microgravity: a possible mechanicsm for bone remodeling. J Appl Physiol 2000;89:1046-54.

23. McCarthy I. The physiology of bone blood flow: a review. J Bone Joint Surg 2006;88 Suppl 3:4-9.

24. Otter MW, Qin YX, Rubin CT, McLeod KJ. Does bone perfusion/reperfusion initiate bone remodeling and the stress fracture syndrome? Medical Hypotheses 1999;53:363-8.

25. McFarlane SI, Muniyappa R, Shin JJ, Bahtiyar G, Sowers JR. Osteoporosis and cardiovascular disease: brittle bones and boned arteries, is there a link? Endocrine 2004;23:1-10.

26. Eriksen EF, Eghbali-Fatourechi GZ, Khosla S. Remodeling and vascular spaces in bone. J Bone Miner Res 2007;22:1-6.

27. Vogt MT, Cauley JA, Kuller LH, Nevitt MC. Bone mineral density and blood flow to the lower extremities: the study of osteoporotic fractures. J Bone Miner Res 1997;12:283-9.

28. Jordan J. Good vibrations and strong bones? Am J Physiol Regul Integr Comp Physiol 2005;288:R555-6.

29. Dyke JP, Aaron RK. Noninvasive methods of measuring bone blood perfusion. Ann N Y Acad Sci 2010;1192:95-102.

30. Lu A, Daniel BL, Pauly JM, Pauly KB. Improved slice selection for R2* mapping during cryoablation with eddy current compensation. J Magn Reson Imaging 2008;28:190-8.

31. Du J, Diaz E, Carl M, Bae W, Chung CB, Bydder GM. Ultrashort echo time imaging with bicomponent analysis. Magn Reson Med 2012;67:645-9.

32. Bashir A, Gray ML, Burstein D. Gd-DTPA2- as a measure of cartilage degradation. Magn Reson Med 1996;36:665-73.

33. Heisen M, Fan X, Buurman J, van Riel NA, Karczmar GS, ter Haar Romeny BM. The influence of temporal resolution in determining pharmacokinetic parameters from DCE-MRI data. Magn Reson Med 2010;63:811-6.

34. Di Giovanni P, Azian CA, Ahearn TS, Semple SI, Gilbert FJ, Redpath TW. The accuracy of pharmacokinetic parameter measurement in DCE-MRI of the breast at 3T. Phys Med Biol 2010;55:121-32.